Design and Evaluation of a Cockpit Display for Hovering Flight

Ronald A. Hess* and Peter J. Gorder†
University of California, Davis, Davis, California 95616

A simulator evaluation of a cockpit display format for hovering flight is described. The display format is based on the position-velocity-acceleration representation similar to that used in the Pilot Night Vision System in the Army AH-64 helicopter. By only varying the nature of the display law driving the "primary" indicator in this format, i.e., the acceleration symbol, three candidate displays are created and evaluated. These range from a status display in which the primary indicator provides true acceleration information, to a command display in which the primary indicator provides flight director information. Simulation results indicate that two of the three displays offer performance and handling qualities that make them excellent candidates for future helicopter cockpit display systems.

Introduction

THE pilots of advanced rotorcraft are being asked to perform increasingly difficult tasks in conditions in which visual out-the-window cues are very poor or nonexistent. Hover and low-speed maneuvering have long been recognized as one of the most workload intensive of such tasks. To aid the pilot in these situations, advanced control and display concepts are being evaluated and utilized.[1] The objective of the study to be described is the modification and evaluation of an existing display format with the goal of improving vehicle handling qualities in a demanding hover task. The display format selected was one currently in operational use in the Army AH-64 Apache attack helicopter. This format is incorporated in a system, called the Pilot Night Vision System (PNVS), and is superimposed on a forward-looking infrared (FLIR) image and presented to the pilot on a helmet-mounted display.[2]

The general format of the PNVS display is shown in Fig. 1. It uses a position-velocity-acceleration (PVA) format in the longitudinal and lateral axes in that distinct symbols on the display present longitudinal and lateral vehicle position (hover pad symbol), vehicle velocity (velocity vector), and a lead indicator for the vehicle velocity (acceleration). The latter symbol in this study will be referred to as a "primary" indicator, and the display laws that drive it varied from the simple status information provided by vehicle acceleration to a combination of vehicle response variables. This combination is obtained via a pilot/vehicle analysis to be described. The resulting display laws are then incorporated in the display of Fig. 1, implemented in a head-up (but not helmet mounted) display, and evaluated in piloted fixed-base simulation.

Numerous display/control system configurations have been investigated to determine their effectiveness in rotorcraft low-speed flight tasks under instrument meteorological conditions.[3] These studies include the variation of display medium, format, and dynamics with different stability and control augmentation systems. The basic PVA display format used here was evaluated recently in a study conducted at NASA Ames Research Center.[4] In Ref. 4, the display medium was a panel-mounted cathode ray tube (CRT) display in the NASA/Army CH-47B variable stability helicopter. The purpose of that study was to investigate the effects of compatible and incompatible display and control system response characteristics and to evaluate a candidate display law design methodology. It is the latter goal that relates directly to the motivation behind this study. A display described in Ref. 4 was used as a benchmark for the candidate display law designs presented herein, and the simulation experiment was designed to maintain consistency with this previous study wherever possible.

Control/Display Laws

Three different display systems differing in the display laws driving the primary indicator were designed and evaluated. They are referred to as 1) the status display, 2) the predictor display, and 3) the command display. Finally, as just noted, the display evaluated in Ref. 4 was used as a benchmark. This display is referred to as the command-status display herein. All of these display types were designed to be flown by the pilot in a similar manner; the pilot moves the cyclic control to drive the "primary indicator" into the hover pad symbol. Thus, the intent of the display designs was to integrate the information that is necessary for hovering flight.

In the status display, the primary indicator is a representation of the rotorcraft's inertial acceleration. In the predictor display, the primary indicator represents a prediction of the position of the tip of the vehicle velocity vector τ_P seconds into the future. In the command display, the primary indicator is essentially a flight director signal, not referenced to the end of the velocity vector. It represents an error in control input that the pilot attempts to null with control motion and can be referenced to the center of the display or the hover pad symbol. As just mentioned, the indicator was referenced to the hover pad symbol in this study.

Three different vehicle response types were investigated: 1) an angular rate-command/attitude hold system (RATE), 2) an attitude-command/attitude hold system (ATTITUDE), and 3) a velocity-command/attitude-hold system (VELOCITY). This is actually an attitude-command/attitude-hold sys-

Received July 28, 1988; presented as Paper 88-4495 at the AIAA/AHS/ASEE Aircraft Design, Systems and Operations Meeting, Atlanta, GA, Sept. 7-9, 1988; revision received March 2, 1989.

*Professor, Department of Mechanical Engineering. Associate Fellow AIAA.

†Graduate Student, Department of Mechanical Engineering. Member AIAA.

Table 1 Control system parameters

	Rate	Attitude	Velocity[a]
M_u	0 rad/ft·s	0 rad/ft·s	0.0152 rad/ft·s
M_q	−2.0 1/s	−2.0 1/s	−3.088 1/s
M_θ	0 1/s^2	−2.0 1/s^2	−2.725 1/s^2
M_{δ_e}	0.21 1/in.·s^2	0.28 1/in.·s^2	0.27 1/in.·s^2
X_u	−0.04 1/s	−0.04 1/s	−0.04 1/s
L_v	0 rad/ft·s	0 rad/ft·s	−0.0198 rad/ft·s
L_p	−2.0 1/s	−2.0 1/s	−3.208 1/s
L_ϕ	0 1/s^2	−2.0 1/s^2	−3.029 1/s^2
L_{δ_a}	0.21 1/in.·s^2	0.28 1/in.·s^2	0.44 1/in.·s^2
Y_v	−0.12 1/s	−0.12 1/s	−0.12 1/s

[a]The parameters listed lead to the following transfer function coefficients in Table 2. Longitudinal: τ_v, 3.33; ζ_v, 1.0; and ω_v, 1.4. Lateral: τ_v, 2.0; ζ_v, 2.0; and ω_v, 1.4.

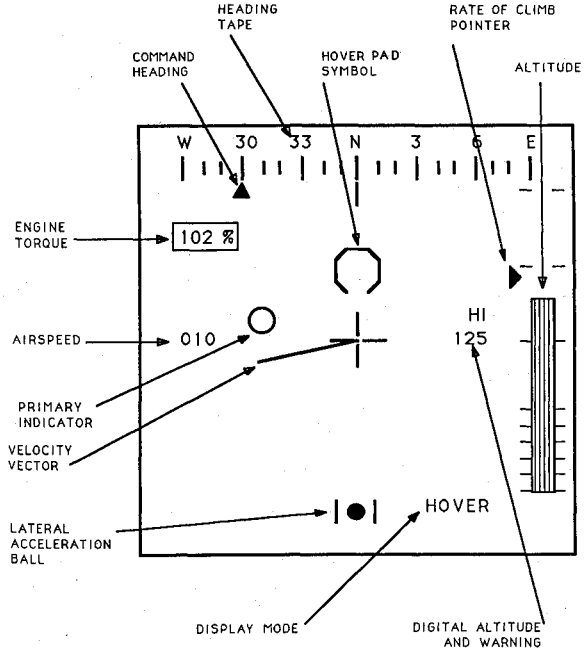

Fig. 1. Position-velocity-acceleration display format.

tem with initial attitude overshoot to quicken the velocity response. The dynamics of these systems were identical to those evaluated in Ref. 4. Table 1 lists the values of the variables shown in Table 2, which create the RATE, ATTITUDE, and VELOCITY control systems, whereas Table 2 shows the vehicle attitude to control transfer functions resulting from each of these feedback implementations. It was these latter control/response dynamic characteristics of Table 2 that were implemented with the model-following flight-control system of the variable stability rotorcraft of Ref. 4 to yield the three fundamental response types just mentioned. It is obvious from the foregoing that the authors are attempting to address some basic control/display issues by using simplified representations of "classical" vehicle response types.

Simulation Tasks

The tasks undertaken in the manned simulation to be described were also identical to those of Ref. 4. Each combination of control/display type is referred to as a "configuration," and each configuration was evaluated in two tasks. The first was a "pad capture" task. Here, the hover pad symbol would undergo an initial step displacement from the center of the display to a new position corresponding to a 60-ft movement of the desired hover point. The pilot was required to fly the vehicle to a stable hover over the new hover point. The

Table 2 Attitude-to-control transfer functions

Rate command

$$\frac{\theta}{\delta_e} = \frac{M_{\delta_e}}{s(s - M_q)}$$

$$\frac{\phi}{\delta_a} = \frac{L_{\delta_a}}{s(s - L_p)}$$

Attitude command

$$\frac{\theta}{\delta_e} = \frac{M_{\delta_e}}{s^2 - M_q s - M_\theta}$$

$$\frac{\phi}{\delta_a} = \frac{L_{\delta_a}}{s^2 - L_p s - L_\phi}$$

Velocity command

$$\frac{\theta}{\delta_e} = \frac{M_{\delta_e}(s - X_u)}{(s + \tau_v)(s^2 + 2\zeta_v\omega_v s + \omega_v^2)}$$

$$\frac{\phi}{\delta_a} = \frac{L_{\delta_a}(s - Y_v)}{(s + \tau_v)(s^2 + 2\zeta_v\omega_v s + \omega_v^2)}$$

Table 3 Sums of sinusoids for pad tracking task

$$x_{\text{pad}} = 5.0\{\sin(0.1841t) + \sin(0.3068t) + \sin(0.4909t) + \sin(0.7977t) + 0.1[\sin(1.166t) + \sin(1.779t) + \sin(2.823t)] + 0.05[\sin(4.663t) + \sin(6.934t)]\} \text{ ft}$$

$$y_{\text{pad}} = 5.0\{\sin(0.2454t) + \sin(0.4295t) + \sin(0.6750t) + \sin(0.9204t) + 0.1[\sin(1.411t) + \sin(2.270t) + \sin(3.743t)] + 0.05[\sin(5.706t) + \sin(7.793t)]\} \text{ ft}$$

second task was a "pad tracking" task in which the hover pad symbol was driven by a sum of sinusoids and the pilot was required to attempt to keep the vehicle over the moving pad. This task can be thought of as tracking a moving ground target. The signals used in the sum of sinusoids are shown in Table 3, and again, are identical to those used in Ref. 4.

Display Law Designs

PVA Format

Since the PVA display format provides the fundamental display layout for all of the displays studied herein, a brief description of the design philosophy behind this format is in order. In the PVA display, the primary indicator can be considered as an acceleration symbol, which is referenced *to the end of the velocity vector symbol.* Thus, if the vehicle were traveling at a constant velocity, its inertial acceleration would be zero, and the acceleration symbol would be positioned on the tip of the velocity vector. The equations governing the position of the acceleration symbol are

$$A_x = K_{sc}(\dot{x} + \ddot{x}) \tag{1a}$$

$$A_y = K_{sc}(\dot{y} + \ddot{y}) \tag{1b}$$

Figure 2a is a graphical representation of Eqs. (1) in terms of actual display format.

The position of the hover pad symbol on the display is determined by the distance between the vehicle and the desired hover point. The vehicle position is always represented by the center of the screen in a "heading-up" mode. The appropriate equations are simply

$$H_x = K_{hv}(x_c - x) \tag{2a}$$

$$H_y = K_{hv}(y_c - y) \tag{2b}$$

where K_{hv} is a display scale factor. Figure 2b is a graphical representation of Eqs. (2) in terms of display format.

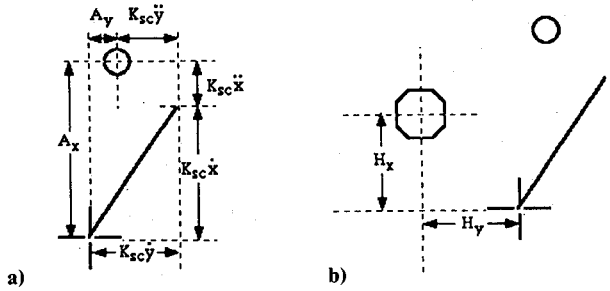

Fig. 2 Display variable definitions.

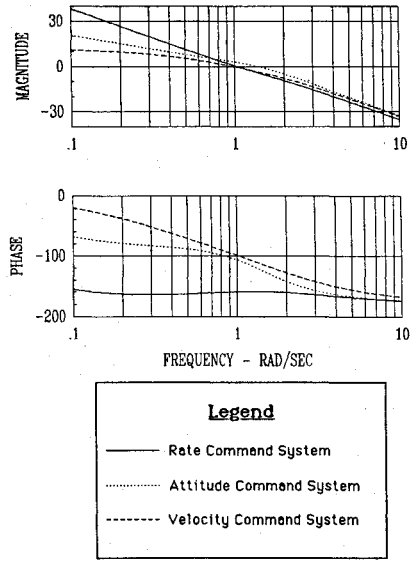

Fig. 3 Primary indicator dynamics for the status display, longitudinal control.

Now consider the vehicle at some initial displacement from a fixed hover pad location, as indicated in Fig. 2b. The piloting strategy of placing and maintaining the acceleration symbol on the hover pad symbol is equivalent to $A_x = H_x$ and $A_y = H_y$ in Eqs. (1) and (2). Considering the solution to the resulting coupled linear differential equations to unit step inputs x_c and y_c yields the following expressions for vehicle position errors as a function of time:

$$x_e(t) = y_e(t) = \left[b/(b-a)\right] \exp(-at) + \left[a/(b-a)\right] \exp(-bt) \tag{3}$$

where

$$a = \left\{1 - \left[1 - (4K_{hv}/K_{sc})\right]^{0.5}\right\}/2 \tag{4a}$$

$$b = \left\{1 + \left[1 - (4K_{hv}/K_{sc})\right]^{0.5}\right\}/2 \tag{4b}$$

Thus, the piloting strategy based on keeping the acceleration symbol on the hover pad symbol would result in an exponential approach to the desired stationary hover position.

Status Design

The PVA display just described, where the primary indicator is driven by Eqs. (1), is referred to here as the status display. Since the task required of the pilot is to place the acceleration symbol on the hover pad symbol and keep it there, the ability

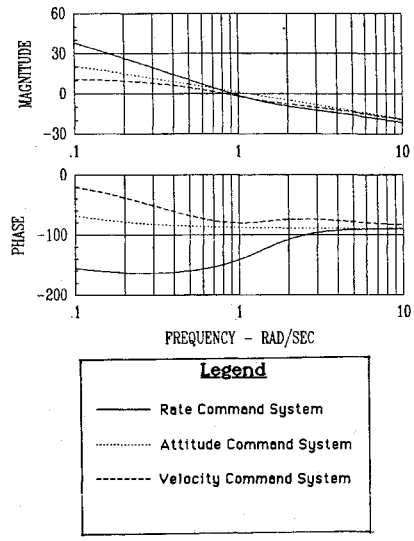

Fig. 4 Primary indicator dynamics for the predictor display, longitudinal control.

of the pilot to accurately control the acceleration symbol is of paramount importance. It is pertinent, therefore, to investigate the relationship between acceleration symbol motion and control inputs. These can be summarized as

$$A_x/\delta_e = \left[-g(s+1)/(s-X_u)\right][\theta/\delta_e] \tag{5a}$$

$$A_y/\delta_a = \left[g(s+1)/(s-Y_v)\right][\phi/\delta_a] \tag{5b}$$

The Bode diagram for A_x/δ_e is shown in Fig. 3 for the three control systems studied. Since the crossover frequencies for these tasks are likely to be above 1 rad/s, the required pilot compensation as predicted by the crossover model of the human pilot[5] will be lead generation, with a lead time constant >1 s. Briefly, the crossover model postulates that the product of the pilot and vehicle transfer functions in single-loop tracking tasks can be approximated by an integrator and time delay in the frequency region around crossover. Lead equalization means increased pilot workload. Similar results hold for the lateral case, which will not be discussed here. Thus, while the strategy of keeping the acceleration symbol on the hover pad is sound, the piloting task of doing so with the status display will be difficult.

Predictor Design

With the predictor display, the primary indicator provides a prediction of the position of the tip of the velocity vector on the vehicle τ_p s in the future. A three-term Taylor series approximation to $x(t+\tau_p)$ was used, which resulted in the following primary indicator dynamics for a prediction time constant of 1 s:

$$A_x = K_{sc}\left\{\dot{x} + \tau_p\ddot{x} - \left[g(\tau_p)^2\ddot{\theta}/\left(2(s-X_u)\right)\right]\right\} \tag{6a}$$

$$A_y = K_{sc}\left\{\dot{y} + \tau_p\ddot{y} + \left[g(\tau_p)^2\ddot{\phi}/\left(2(s-Y_v)\right)\right]\right\} \tag{6b}$$

$$A_x/\delta_e = \left[-g(0.5s^2+s+1)/(s-X_u)\right][\theta/\delta_e] \tag{6c}$$

$$A_y/\delta_a = \left[g(0.5s^2+s+1)/(s-Y_v)\right][\phi/\delta_a] \tag{6d}$$

The Bode diagram for A_x/δ_e is shown in Fig. 4 for the three control systems studied. In terms of the required pilot equal-

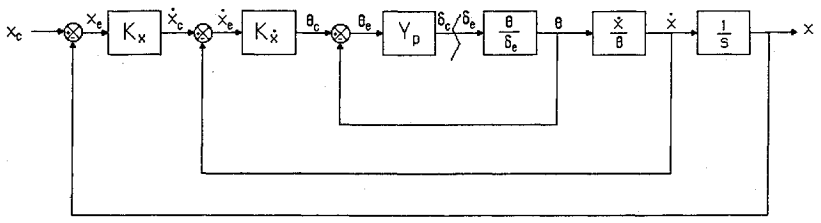

Fig. 5 Pilot-loop closures in a hover task.

ization, things are improved considerably over the status display as only pure gain equalization is required of the pilot for crossover frequencies above 1.0 rad/s. Indeed, the prediction time constant of 1 s was chosen so as to create this desirable characteristic.

Command Display

The command display differs from the status and predictor displays in that it is based on a flight-director design philosophy. As implemented here, the command display law for the primary indicator was obtained by considering the control strategy that the pilot would use in the pad tracking task and then providing a cyclic command through the acceleration symbol on the display that is based on this strategy. This general flight director design approach is discussed in Ref. 6.

The piloting strategy and the flight director design philosophy emanate from a consideration of Fig. 5, which is a block diagram representation of the loop closures that a pilot would employ in controlling the longitudinal position of the vehicle without the aid of a special display. A similar diagram could be drawn for the lateral mode. Here, three loops are closed involving the control of vehicle attitude, velocity, and position, respectively. The hypothesis here is that, *for the purposes of command display design,* the loop closure sequence shown in Fig. 5 would be used by the pilot for *all* the vehicle response types studied herein including the velocity command system. Further, it is the hypothesis that the pilot closes each successive loop so as to obtain K/s characteristics for that loop and whatever inner loops it contains.

Each loop closure in Fig. 5 is modeled by an application of the crossover model of the human pilot, with crossover frequencies differing by a factor of 2 between successive loops. Whereas a factor of 3–4 is usually assumed in multiloop modeling problems (e.g., Ref. 6), the factor of 2 was chosen to provide a command display suited to the demands of the pad tracking task, i.e, the relatively high frequency content of the sum of sinusoids driving the hover pad symbol. In single axis laboratory tracking tasks, crossover frequencies on the order of 3–5 rad/s are typical, depending on the controlled element dynamics and the input bandwidth.[5] Because this experiment was multiaxis in nature, a nominal attitude loop crossover frequency of 2 rad/s was assumed. The crossover frequencies in the velocity and position loops then become 1 and 0.5 rad/s, respectively.

As Table 2 indicates, the attitude to control transfer functions for all the response types were approaching second order in the region of crossover. The pilot model for the command display design was thus chosen of the form $Y_p = K_p(Ts+1)$. The lead time constant T was chosen to force K/s-like amplitude characteristics in the open-loop pilot/vehicle transfer function around crossover and K_p was chosen to give the desired crossover frequency. Because the subsequent control loops for both the longitudinal and lateral cases are assumed to involve effective controlled element dynamics that are K/s-like around the respective outer loop crossover frequencies, the pilot transfer functions for these closures can be just pure gains $K_{\dot{x}}$ and K_x, selected to give the desired crossover frequencies.

Using Fig. 5 and a similar diagram for lateral control, the following expressions for the pilot control inputs result:

$$\delta e_c = K_{\dot{x}}K_x Y_p(x_c - x) - K_{\dot{x}}Y_p\dot{x} - (Y_p\theta_{wo}) \tag{7a}$$

$$\delta a_c = K_{\dot{y}}K_y Y_p(y_c - y) - K_{\dot{y}}Y_p\dot{y} - (Y_p\phi_{wo}) \tag{7b}$$

The similarity between the longitudinal and lateral attitude dynamics allowed inner-loop pilot dynamics Y_p, which differed only in the gain K_p to be used for the two axes for each response type. θ_{wo} and ϕ_{wo} refer to pitch and roll-attitude passed through a first order washout filter with a 20 s time constant to remove changing trim effects.

The command display can now be created by simply implementing Eqs. (7) as a *display law,* and driving the primary indicator by variables A_x and A_y, which are now nothing more than δe_c and δa_c, appropriately scaled. Thus, the position of the primary indicator relative to some null position on the display screen provides longitudinal and lateral cyclic commands to the pilot. To provide a common control strategy across the different display types, the null position for the primary indicator for the command display was chosen as the hover pad symbol itself. In addition, the scaling of the primary indicator had to be chosen so that the instantaneous pad displacement at the beginning of the pad capture task did not cause primary indicator movement. This was accomplished by using the same scaling for the primary indicator as for the hover pad symbol for pure position error.

The primary indicator dynamics for the command display can be given as

$$A_x = K_{\text{mod}}\Big\{K_{gx}\Big[K_{px}\Big(s+(1/T)\Big)(-K_xK_{\dot{x}}x - K_{\dot{x}}\dot{x} - \theta_{wo})\Big] - H_x\Big\} \tag{8a}$$

$$A_y = K_{\text{mod}}\Big\{K_{gy}\Big[K_{py}\Big(s+(1/T)\Big)(-K_yK_{\dot{y}}y - K_{\dot{y}}\dot{y} - \phi_{wo})\Big] - H_y\Big\} \tag{8b}$$

$$A_x/\delta_e = \Big\{K_{px}\Big[s+(1/T)\Big]\Big[s^3 - (X_u + gK_{\dot{x}})s^2 - gK_{\dot{x}}\Big((1/\tau_{wo}) + K_x\Big)s - (gK_{\dot{x}}K_x)/\tau_{wo}\Big]\Big\}\Big/\Big[s(s-X_u)(s+1/\tau_{wo})\Big] \tag{8c}$$

$$A_y/\delta_a = \Big\{K_{py}\Big[s+(1/T)\Big]\Big[s^3 + (-Y_v + gK_{\dot{y}})s^2 + gK_{\dot{y}}\Big((1/\tau_{wo}) + K_y\Big)s + (gK_{\dot{y}}K_y)/\tau_{wo}\Big]\Big\}\Big/\Big[s(s-Y_v)(s+1/\tau_{wo})\Big] \tag{8d}$$

Here, τ_{wo} is the 20 s attitude washout time constant just men-

tioned. The Bode diagram for the A_x/δ_e transfer functions are shown in Fig. 6 for each of the control response types. Note the desirable K/s-like characteristics.

Command-Status Display

The philosophy behind the command-status design is discussed in Ref. 4 and will not be treated here. Like the command display, it is based on a flight director concept, but with different primary indicator dynamics. The Bode diagram for the A_x/δ_e transfer functions are shown in Fig. 7 for each of the control response types. Note that, as compared to the diagrams of Fig. 6, the command-status display dynamics are not K/s-like in the hypothesized crossover region. The flat amplitude characteristics for frequencies beyond 1 rad/s indicate that the pilot would be required to generate lag equalization for crossover frequencies above 1 rad/s. It should be noted that these display dynamics were felt to be acceptable to the pilots in Ref. 4.

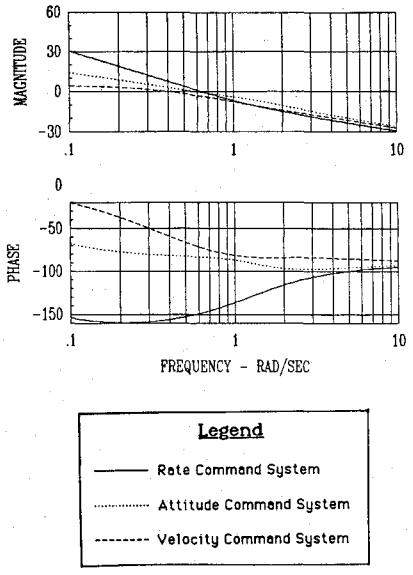

Fig. 6 Primary indicator dynamics for the command display, longitudinal control.

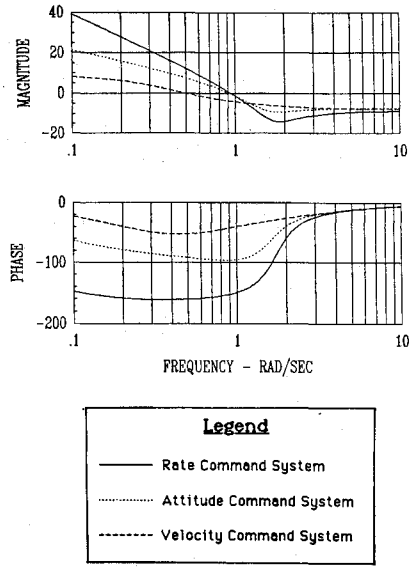

Fig. 7 Primary indicator dynamics for the command-status display, longitudinal control.

Figures 8 and 9 list the parameter values for Eqs. (7) and (8) in addition to the display scaling constant K_{sc} for each display and control response type. The degrees appearing in the numerator of the units for the constant K_{sc} are "screen" degrees, a unit peculiar to the particular display implementation. Again it is worth emphasizing that, in terms of format, *all* the display designs just discussed are *identical* and appear to the pilot as shown in Fig. 1.

Simulation

The experimental matrix for the manned simulation consisted of 24 elements involving four display types and three control response types for each of the two tasks involved. A NASA Ames fixed-base simulator was used in the experimental study. The simulator has a computer-generated terrain image, visible on a 2×2 ft window in the cockpit. The head-up display symbology of Fig. 1 was projected onto this window using a half silvered mirror. Both the terrain image and display

	RATE	ATTITUDE	VELOCITY
Status			
K_{sc}	.256 deg/ft/sec	.256 deg/ft/sec	.256 deg/ft/sec
K_{sc}	.256 deg/ft/sec	.256 deg/ft/sec	.256 deg/ft/sec
Predictor			
K_{sc}	.256 deg/ft/sec	.256 deg/ft/sec	.256 deg/ft/sec
τ_p	1.0 sec	1.0 sec	1.0 sec
X_u	-.04 1/sec	-.04 1/sec	-.04 1/sec
K_{sc}	.256 deg/ft/sec	.256 deg/ft/sec	.256 deg/ft/sec
τ_p	1.0 sec	1.0 sec	1.0 sec
Y_v	-.12 1/sec	-.12 1/sec	-.12 1/sec

Fig. 8 Display-law parameter values, status and predictor displays.

	RATE	ATTITUDE	VELOCITY
Command			
K_{gx}	-0.1677 deg/in	-0.2793 deg/in	-0.1853 deg/in
K_{p_x}	9.573 in/rad	6.268 in/rad	8.744 in/rad
$K_{\dot{x}}$	-0.0263 rad/ft/sec	-0.0361 rad/ft/sec	-0.0380 rad/ft/sec
K_x	0.5476 1/sec	0.5173 1/sec	0.531 1/sec
τ_{wo}	20.0 sec	20.0 sec	20.0 sec
T	0.50 sec	0.707 sec	0.707 sec
K_{mod}	1. unmod./2. mod.	1. unmod./2. mod.	1. unmod./2. mod.
K_{gy}	0.1554 deg/in	0.2588 deg/in	0.2646 deg/in
K_{p_y}	9.573 in/rad	6.268 in/rad	5.461 in/rad
$K_{\dot{y}}$	0.0265 rad/ft/sec	0.0363 rad/ft/sec	0.0399 rad/ft/sec
K_y	0.5864 1/sec	0.555 1/sec	0.567 1/sec
τ_{wo}	20.0 sec	20.0 sec	20.0 sec
T	0.50 sec	0.707 sec	0.707 sec
K_{mod}	1. unmod./2. mod.	1. unmod./2. mod.	1. unmod./2. mod.

Fig. 9 Display-law parameter values, command display.

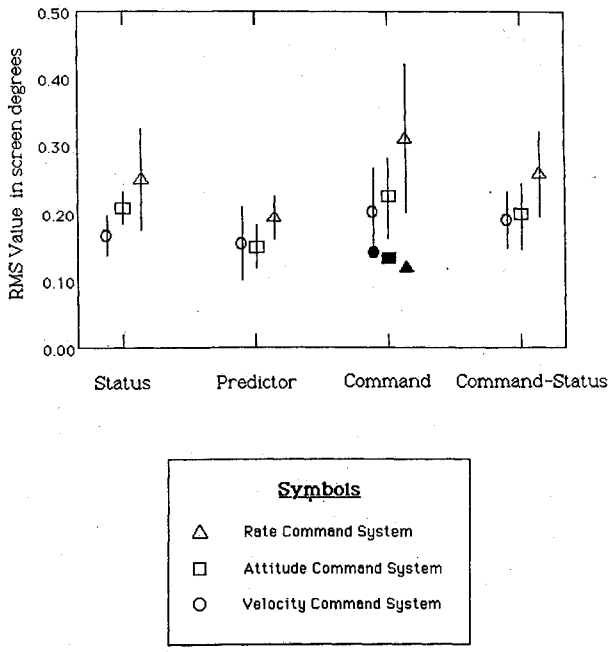

Fig. 10 Pilot/vehicle performance, primary indicator error.

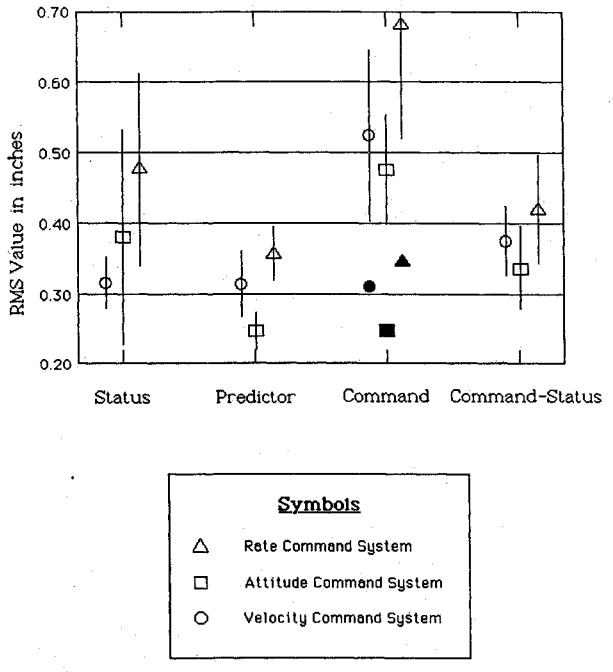

Fig. 11 Pilot/vehicle performance, longitudinal cyclic input.

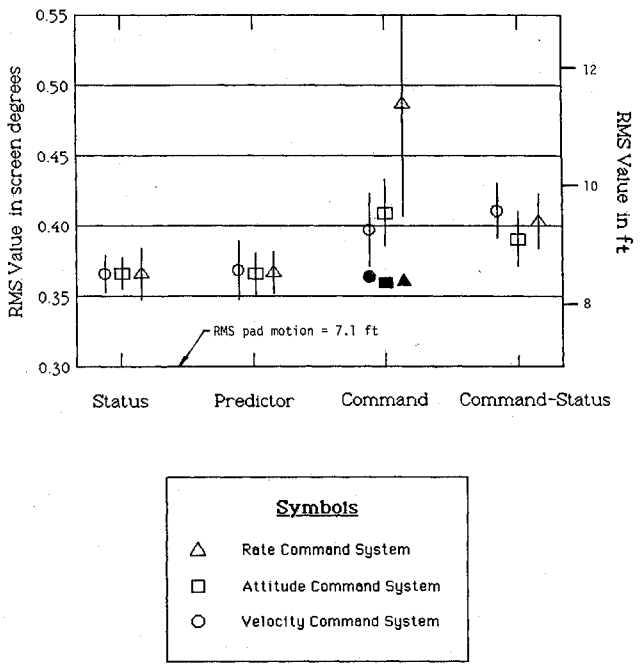

Fig. 12 Pilot/vehicle performance, longitudinal position error.

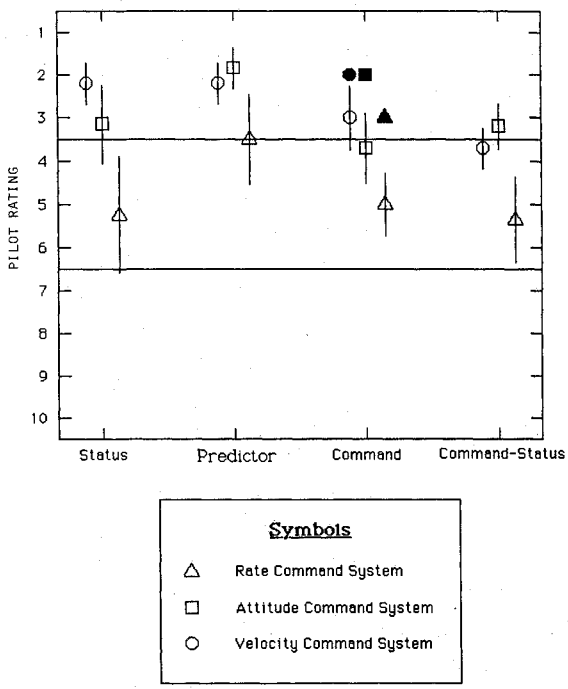

Fig. 13 Cooper-Harper ratings, pad capture task.

were focused at infinity. Four NASA test pilots participated in the simulation.

In each of the tasks, criteria of desired and adequate performance were communicated to the pilots.

Pad Capture Task

1) Desired performance: Limit overshoot to 7.5 ft (within displayed hover pad). Maintain hover within 7.5 ft (within displayed hover pad). Maintain altitude within 20 ft. Stabilize in hover within 8 s of starting task.

2) Adequate performance: Twice the values for desired performance.

Pad Tracking Task

1) Desired performance: Maintain position relative to hover pad to within 7.5 ft. Maintain altitude within 10 ft. Maintain heading within 5 deg.

2) Adequate performance: Twice the values for desired performance.

Two different types of simulation sessions were organized for each of the pilots. The first was a performance session and the second a handling qualities rating (HQR) session. In the latter, the Cooper-Harper pilot rating scale was used.[7] In presenting the configurations to each pilot, no two consecutive configurations were presented with the same display type or

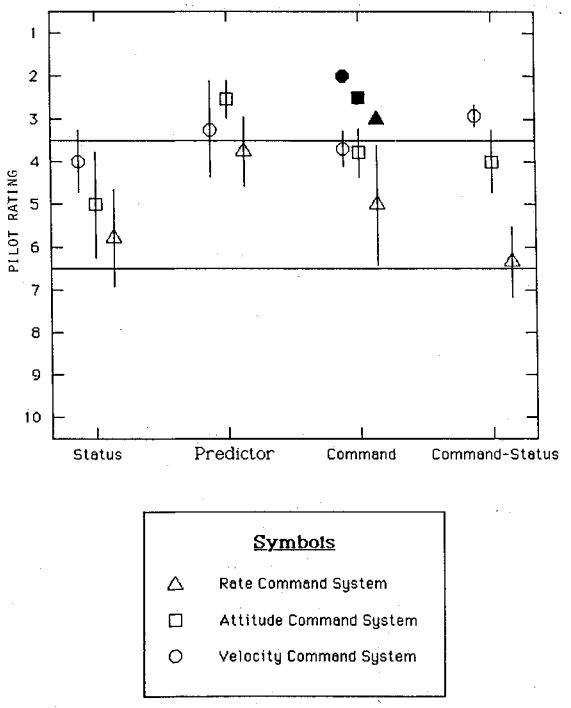

Fig. 14 Cooper-Harper ratings, pad tracking task.

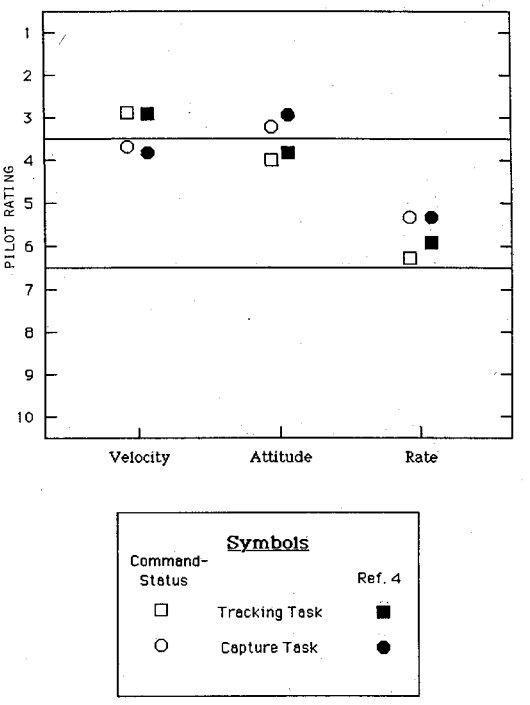

Fig. 15 Pilot rating comparison for the benchmark command-status and the equivalent display used in flight in Ref. 4.

control system response type. Three different schedules of such presentations were created. In the performance session, each configuration was run four times in succession. The first three runs were pad capture tasks with the last being a 2-min pad tracking task. In the pad capture task, the pad was displaced first in the x direction (vertically on the display), then the y direction (horizontally to the right on the display), then in a random azimuth direction. In all, three sets of such performance runs were required of each pilot. Although four pilots were used in the simulation, only three were able to contribute full data sets, which consisted of three performance sessions and one ratings session. The fourth pilot completed only one data taking session but did complete the rating session.

Results

Figures 10–14 summarize the performance data for the pad tracking task and the handling qualities data for both the pad tracking and pad capture tasks across display control laws and control response types. For brevity, only performance data for longitudinal control in the pad tracking task is presented. The vertical bars in these figures represent twice the standard deviations of the variables presented. Of particular interest here are the shaded symbols. The initial command display was rated rather poorly, and pilot comments indicated that the pilots objected to the large attitude excursions that accompanied command display use. The shaded symbols represent performance and ratings for the command display with a modified null position, which was on an imaginary line through the center of the display and the hover pad symbol but at twice the distance of the pad from the screen center. The location of the new null position was unknown to the pilot and of no consequence in the tasks. The pilot was still instructed to place the primary indicator on the pad symbol and simply noticed that smaller control inputs and vehicle attitudes were needed to accomplish this than previously required. A single pilot was used to evaluate the modified command display. As can be seen from the figures, the modified command display resulted in a significant improvement in performance and ratings.

In Figs. 10–14, three results clearly stand out. Namely, for the tasks studied here, 1) the predictor and command designs emerge as superior display candidates, 2) the RATE response system does not offer adequate stability and control augmentation, and 3) as the control response type increases in sophistication, performance and ratings are less dependent upon display type. This result is consistent with the results of past research on control/display tradeoffs (e.g., Ref. 3).

Figure 15 compares the ratings obtained with the command-status display of this experiment with those obtained from the equivalent display in flight and reported in Ref. 4. The comparisons are seen to be excellent. This is particularly noteworthy given the limitations of the fixed-base simulator. This excellent comparison is probably due to three factors: First, the vehicle dynamics simulated both in the laboratory and in flight were relatively simple in form, as was the control augmentation used to obtain the response types. Second, the flight task used a head-down display so that visual field cues were not used in flight. Finally, the task itself was well defined and centered on use of the primary indicator in the cockpit displays.

Conclusions

Based on the analytical and experimental study summarized herein, the following specific conclusions can be drawn.

1) The predictor and command displays offer excellent performance and handling qualities in both the pad tracking and capture tasks. Both displays should be serious candidates for inclusion in future helicopter cockpit display systems.

2) The effect of the scaling of the primary indicator is very important and should be taken into account in the design process. When superior display dynamics are coupled with poor scaling, both pilot opinion and performance suffer considerably.

3) With increased vehicle control augmentation, the dynamics of the primary indicator become less critical. This is due to the decrease in pilot workload brought about by the higher levels of augmentation.

Acknowledgements

This work was performed under NASA Ames Research Center Grant NCC2-383. The advice and assistance of Mr.

Edwin Aiken of Boeing Vertol Co. and Dr. J. Victor Lebacqz of the Flight Dynamics and Controls Branch at NASA Ames Research Center are deeply appreciated.

References

[1]Aiken, E. W., and Merrill, R. K., "Results of a Simulator Investigation of Control System and Display Variations for an Attack Helicopter Mission," AHS Preprint No. 80-28, American Helicopter Society 36th Annual National Forum, Washington, DC, May, 1980.

[2]Tsoubanos, C. M., and Kelley, M. B., "Pilot Night Vision System (PNVS) for Advanced Attack Helicopter (AAH)," American Helicopter Society 34th Annual National Forum, Washington, DC, May 1978.

[3]Lebacqz, J. V., "Survey of Helicopter Control/Display Investigations for Instrument Decelerating Approach," NASA TM-78565, 1979.

[4]Eshow, M. M., Aiken, E. W., and Hindson, W. S., "Preliminary Results of a Flight Investigation of Rotorcraft Control and Display Laws for Hover," American Helicopter Society Mideast Regional National Specialists' Meeting in Rotorcraft Flight Controls and Avionics, Cherry Hill, NJ, Oct. 1987.

[5]McRuer, D. T., and Krendel, E. S., "Mathematical Models of Human Pilot Behavior," AGARDograph 188, Jan. 1974.

[6]Hess, R. A., and McNally, B. D., "Automation Effects in a Multiloop Manual Control System," *IEEE Transactions on Systems, Man, and Cybernetics,* Vol. SMC-16, No. 1, 1986, pp. 111-121.

[7]Cooper G. E., and Harper, R. P., Jr., "The Use of Pilot Rating in the Evaluation of Aircraft Handling Qualities," NASA TN-D-5133, April 1969.